Si(111)-($\sqrt{3}\times\sqrt{3}$)Ag Surface Structure Studied by Impact-Collision Ion-Scattering Spectrometry

T. L. Porter, C. S. Chang, and I. S. T. Tsong
Department of Physics, Arizona State University, Tempe, Arizona 85287
(Received 23 November 1987)

Using the technique of impact-collision ion-scattering spectrometry, we showed that the geometry of the Si(111)-($\sqrt{3}\times\sqrt{3}$)Ag surface consists of Si honeycomb on top of Ag trimers. The separation of the Si and Ag layers is 0.7 ± 0.3 Å and the Si–Ag bond length is 2.73 ± 0.3 Å. We also observed, for the first time, type-A and type-B arrangements of the Si and Ag atoms on the surface, with type B being type A rotated 180° about the surface normal.

PACS numbers: 61.16.Fk, 68.35.Bs

When a few monolayers (ML) of Ag are deposited onto a clean Si(111) 7×7 surface which is annealed at ~300°C, the familiar ($\sqrt{3}\times\sqrt{3}$)$R30°$ LEED pattern appears. Scanning-electron-microscopy studies[1] show that Ag crystallites begin to form as deposition continues, but since they only cover a fraction of the surface, the $\sqrt{3}$ LEED pattern persists even at higher coverages. The structure and stoichiometry of the Si(111)-($\sqrt{3}\times\sqrt{3}$)Ag surface have been extensively studied in recent years, resulting in a variety of models proposed for the structure of the $\sqrt{3}$ surface for coverages of $\frac{1}{3}$, $\frac{2}{3}$, and 1 ML of Ag. Ever since Le Lay, Manneville, and Kern[2] proposed the honeycomb model for the $\sqrt{3}$ structure at $\frac{2}{3}$-ML coverage, other experiments followed,[3-8] providing evidence for a Ag honeycomb structure either residing on top of the Si or embedded in the first double layer of Si. Recently, the honeycomb geometry was unequivocally confirmed by scanning-tunneling-microscopy (STM) images.[9,10] However, the interpretation of STM images led to two different conclusions: (a) Ag trimers are situated below the topmost layer of Si atoms which have a honeycomb geometry,[9] and (b) Ag atoms in a honeycomb geometry reside on top of the Si atoms.[10] In the present report, we resolve the issue by studying the Si(111)-($\sqrt{3}\times\sqrt{3}$)Ag surface with the technique of impact-collision ion-scattering spectrometry (ICISS)[11,12] which has the advantage of providing information on both atomic composition and in-plane geometry of the surface layers.

The experiments were carried out in an ultrahigh-vacuum chamber fitted with a reverse-view LEED, two electrostatic energy analyzers, an electron-beam deposition unit, and a Colutron ion-beam system.[13] After removal of the native oxide layer by chemical etching, the *n*-type Si(111) wafer with 0.02 Ω cm resistivity was mounted on a precision manipulator equipped with electron-beam heating and liquid-nitrogen cooling of the sample. Base pressure was 1×10^{-10} Torr or lower. The surface was annealed at 1000°C for 2 min after being sputtered briefly by 3-keV Ar^+ ions. Such surface treatment consistently produced sharp 7×7 LEED patterns. 3 Å (~2 ML) of Ag were deposited onto the Si substrate which was then annealed at 300°C for 2 min, resulting in the $\sqrt{3}\times\sqrt{3}$ LEED pattern. In the ICISS mode, 1-keV He^+ primary ions scattered from either Ag (at 864 eV) or Si (at 562 eV) were detected at a scattering angle of 163°, which is close to the ideal 180°. Polar scans were performed by rotation of the sample from 0° incident angle, i.e., beam parallel to the surface, to 50° in 2° increments.

The counting rates for He^+ ions scattered off Ag atoms were sufficiently high that exposure of the surface to the He^+-ion beam for a complete polar scan took less than 4 min. No significant surface damage was observed during this period. However, the counting rates for ions scattered from Si atoms were considerably lower because of the lower scattering cross section of the Si atom. For this reason, the dwell time of the ion beam at each polar angle during the Si scans was doubled. Because of the longer exposure of the surface to the ion beam, the effect of surface damage was such that the sample had to be reannealed at ~250°C for 2 min midway through the polar scan to restore the $\sqrt{3}\times\sqrt{3}$ LEED pattern before continuation of the scan.

In ICISS, the blocking effect is negligible and only the shadowing effect is taken into account. To check our calculated shadow cones,[14] 20 Å (15 ML) of Ag were deposited on Si(111) and annealed at ~200°C for 5 min to obtain the (1×1) LEED pattern. ICISS polar scans along $[\bar{1}10]$ and $[11\bar{2}]$ azimuths were taken with a 1-keV He^+ primary ion beam. The critical angles for the shadowing of Ag atoms at $20°\pm1°$ for $[\bar{1}10]$ and at $13°\pm1°$ for $[11\bar{2}]$ agree well with theoretical values of 21° for $[\bar{1}10]$ and 13° for $[11\bar{2}]$ calculated with a screening-length scaling factor of 0.9.[14]

The experimental ICISS polar scans of scattered Ag and Si intensities shown in Figs. 1 and 2, respectively, are compared with computer-simulated scans performed for the embedded Ag trimer[9] and Ag honeycomb[10] models. The peaks in the polar scans occur as a result of the so-called "focusing" effect when the shadow cone edge just passes the atom where scattering takes place. In our

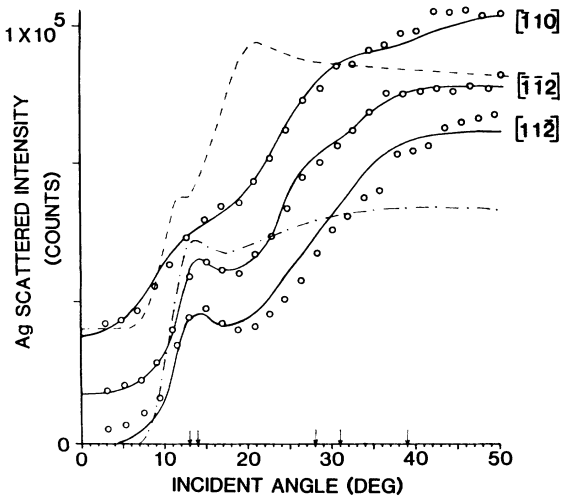

FIG. 1. ICISS polar-angle scan for 1-keV He^+ ions backscattered from Ag atoms along $[\bar{1}10]$, $[11\bar{2}]$, and $[\bar{1}\bar{1}2]$ azimuths (circles). The computer simulation of the backscattered intensity is shown as solid curves for the embedded-Ag-trimer model and broken curves for the Ag-honeycomb model. The data points and curves for the different azimuths are displaced for clarity. The arrows indicate positions of shadow-focusing peaks.

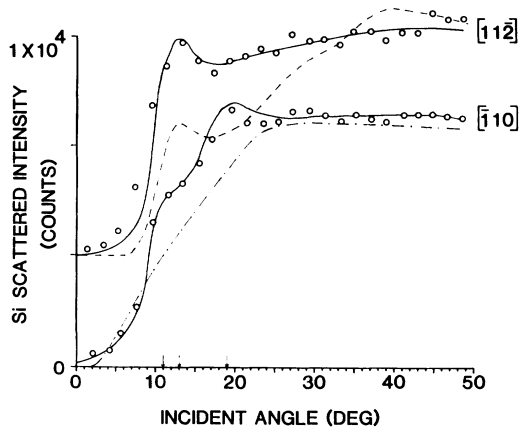

FIG. 2. ICISS polar-angle scan for 1-keV He^+ ions backscattered from Si atoms along $[11\bar{2}]$ and $[\bar{1}10]$ azimuths (circles). The computer simulation of the backscattered intensity is shown as solid curves for the embedded-Ag-trimer model and broken curves for the Ag-honeycomb model. The data points and curves for the two different azimuths are displaced for clarity. The arrows indicate positions of shadow-focusing peaks.

computer simulation, the backscattered intensity is represented by the hitting probability in a two-atom model[15] where the deflection angle as a function of impact parameter is calculated with use of the Thomas-Fermi-Molière potential with a screening-length scaling factor of 0.9.[14] Because of the extremely high neutralization efficiency for low-energy noble-gas ions, only the top two layers of the surface were considered in the simulations. The thermal vibration amplitudes of surface atoms are 0.15 Å for Si in the embedded-trimer model and 0.13 Å for Ag in the honeycomb model. The characteristic velocity v_0 in the neutralization factor $\exp(-v_0/v)$ is taken to be 5×10^7 cm/s for scattering from Ag and 3×10^7 cm/s for scattering from Si to obtain best fit with the embedded-Ag-trimer model. Our attempt to fit the experimental data with the Ag-honeycomb model turned out to be very difficult. Even with the use of unrealistic values of the neutralization factor, the fits were not satisfactory. The computer simulations shown in Figs. 1 and 2 for the Ag-honeycomb model were performed with characteristic velocities of 3.3×10^7 cm/s for scattering from Ag and 4.5×10^7 cm/s for scattering from Si, which probably produced the best possible overall fits.

Figure 1 shows the ICISS experimental polar scans for Ag (circles) along the $[\bar{1}10]$, $[11\bar{2}]$, and $[\bar{1}\bar{1}2]$ azimuths. The computer-simulated scans for these azimuths are shown as continuous curves for the embedded-Ag-trimer model[9] and broken curves for the Ag honeycomb model.[10] It is immediately obvious that the embedded-Ag-trimer model provides better agreement with experimental data. The general trend of the ICISS scans in Fig. 1, i.e., high counts at high angles of incidence with a gradual decrease in counts as the beam becomes more parallel to the surface, is indicative that the Ag atoms do not reside on the topmost layer. In polar scans along $[11\bar{2}]$ and $[\bar{1}\bar{1}2]$ azimuths (Fig. 1), the Ag-Ag spacing is 6.65 Å apart (Fig. 3) and the Ag self-shadowing occurs at an incident (polar) angle of 14°. From the top view of Fig.

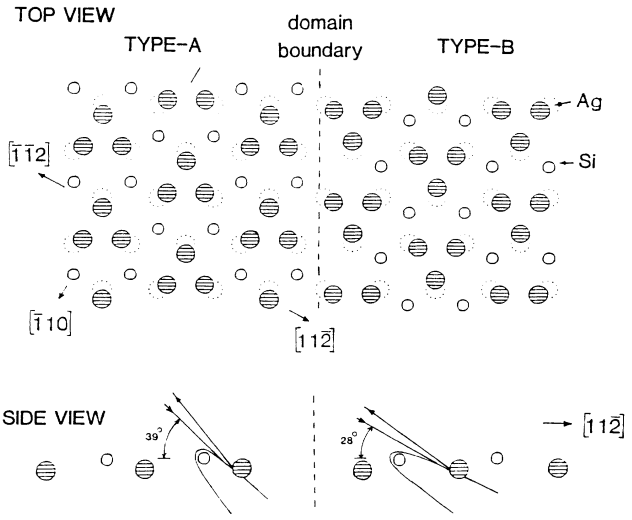

FIG. 3. Model of the top two layers of the Si(111)-$(\sqrt{3}\times\sqrt{3})$Ag surface showing the type-A and type-B embedded-Ag-trimer structure. The Ag trimers in the second layer show a slight reconstruction by collapsing 0.7 Å toward the center of the trimer. The distance between the Si and Ag layers is 0.7 ± 0.3 Å by computer simulation to obtain best fit with experimental data.

3, the Si-Ag spacing is 2.57 Å along $[11\bar{2}]$ azimuth and 4.08 Å along $[\bar{1}\bar{1}2]$. Thus the shadowing of Ag by Si is expected to occur at 39° incident angle for $[11\bar{2}]$ and at 28° for $[\bar{1}\bar{1}2]$. However, from the polar scans in Fig. 1, it can be seen that Si-Ag shadowing occurs at both 39° and 28° for both azimuths. In the top view shown in Fig. 3, if we define a type-B surface structure consisting of the type-A structure rotated 180° about the surface normal, then the Si-Ag spacing along $[11\bar{2}]$ azimuth is 2.57 Å for type A and 4.08 Å for type B. If we further assume a 60% type-A and 40% type-B mixture, then computer simulations show shadow-focusing peaks at 39° and 28° for both azimuths. In the computer-simulated scans (continuous curves) shown in Fig. 1, the 39° peak is more prominent for $[11\bar{2}]$ azimuth, whereas the 28° peak is more prominent for $[\bar{1}\bar{1}2]$ azimuth because of the type-A structure being 60%. For our computer simulation, we also find that a distance of 0.7 ± 0.3 Å between the top Si and Ag layers provides the beast agreement with the experimental data. Furthermore, we allow the Ag trimer to collapse toward its center as a result of the mutual attraction of the Ag atoms; thus the Ag atom (shaded circle) now sits 0.7 Å away from its ideal position (dotted circle) as shown in Fig. 3. This means that along the $[11\bar{2}]$ and $[\bar{1}\bar{1}2]$ azimuths, the Si and Ag atoms are slightly offset from each other, which explains the somewhat nondistinct shadowing peaks at 39° and 28° polar angle (Fig. 1).

In the polar scan along the $[\bar{1}10]$ azimuth (Fig. 1), only Ag self-shadowing occurs. The Ag-Ag spacing of 2.63 Å along this azimuth gives rise to a shadowing peak at 31° polar angle. The other Ag-Ag spacing, 4.45 Å, only provides a broad shoulder from 13° to 19° rather than a distinct peak because the Ag atoms at this spacing are offset as a result of the contraction of the trimer as shown in Fig. 3. The computer-simulated scan (continuous curve) agrees very well with experiment.

Figure 2 shows the ICISS experimental polar scans for Si (open circles) along $[11\bar{2}]$ and $[\bar{1}10]$ azimuths with computer-simulated scans shown as continuous curves for the embedded-Ag-trimer model[9] and broken curves for the Ag-honeycomb model.[10] Similar to the polar scans for Ag, the embedded-trimer model provides much better agreement with experiment than the Ag-honeycomb model. Along the $[11\bar{2}]$ azimuth, only Si self-shadowing operates on the topmost layer according to Fig. 3 regardless of whether it is type-A or type-B structure. This results in the only shadowing peak at 13° polar angle (Fig. 2) which corresponds to a Si-Si spacing of 6.65 Å. Along the $[\bar{1}10]$ azimuth, once again only Si self-shadowing is in effect (Fig. 3), resulting in two shadowing peaks in the polar scan (Fig. 2) at 19° and 11° which correspond to Si-Si spacings of 3.84 and 7.68 Å, respectively.

Our ICISS results thus indicate that at least in the top two layers of the Si(111)-$(\sqrt{3}\times\sqrt{3})$Ag surface, the Si atoms reside on the topmost layer arranged in a honeycomb structure while the Ag atoms reside in a second layer with a slightly reconstructed trimer structure as shown in Fig. 3. The separation of these two layers is 0.7 ± 0.3 Å and the Si–Ag bond length is 2.73 ± 0.3 Å according to our computer simulation.

It must be mentioned that Aono *et al.*[16] also performed ICISS measurements with a 1-keV Li^+-ion beam on Si(111)-$(\sqrt{3}\times\sqrt{3})$Ag. They reported polar scans of scattering from Ag only and proposed the Ag-honeycomb model as the best description of their data. We performed a computer simulation of their polar scan along the $[11\bar{2}]$ azimuth and found that their data agree with the model of embedded Ag trimer with Si honeycomb on top. The separation of the two layers, however, is only 0.2 Å compared with 0.7 Å in the present work. Their $[\bar{1}10]$ polar scan does not yield such good agreement with the embedded-Ag-trimer model, but this could be due to the amount of zig-zag and multiple scattering of the Li^+ ion along this azimuth, which makes computer simulation considerably more difficult than He^+-ion scattering.

Most recently, Wilson and Chiang[17] have observed domains of Si(111)-$(\sqrt{3}\times\sqrt{3})$Ag structure at the edges of pristine 7×7 terraces with sharp domain boundaries. From their STM images, they conclude that the honeycomb protrusions occur at H_3 sites, which is not consistent with the embedded-trimer model.[9] Our ICISS results show that the top two layers have the arrangement of Si honeycomb on top of Ag trimers. To interpret our results in terms of the STM images of Wilson and Chiang,[17] the Ag atoms are substitutional atoms, residing on sites previously occupied by the top Si atoms on the Si(111) 7×7 surface, forming a trimer structure; while the top Si atoms sit on H_3 sites arranged in a honeycomb structure. A more precise description of our model shown in Fig. 3 should thus be "substitutional trimer" rather than "embedded trimer" since the word "embedded" implies that the Ag atoms diffuse into the first double layer of Si. With our present ICISS setup, we could not determine the structure of third or fourth Si layers because of neutralization of the He^+ ions. Further experiments with ICISS using time-of-flight detection combined with three-dimensional computer simulation may be useful for a complete characterization of this interesting surface.

This work was supported by the National Science Foundation under Grant No. DMR-8412232. We greatly appreciate many helpful discussions with J. E. Northrup on this problem.

[1]J. A. Venables, J. Derrien, and A. P. Janssen, Surf. Sci. **95**, 411 (1980).

[2]G. Le Lay, M. Manneville, and R. Kern, Surf. Sci. **72**, 405 (1978).

[3]M. Saitoh, F. Shoji, K. Oura, and T. Hanawa, Surf. Sci. **112**, 306 (1981).

[4]D. Bolmont, P. Chen, and C. A. Sebenne, J. Phys. C **14**, 3313 (1981).

[5]Y. Terada, T. Yoshizuka, K. Oura, and T. Hanawa, Surf. Sci. **114**, 65 (1982).

[6]J. Stohr, R. Jeager, G. Rossi, T. Kendelewicz, and I. Lindau, Surf. Sci. **134**, 813 (1983).

[7]F. Houzay, G. M. Guichar, A. Cros, F. Salvan, R. Pinchaux, and J. Derrien, Surf. Sci. **124**, L1 (1983).

[8]S. Kono, H. Sakurai, K. Higashiyama, and T. Sagawa, Surf. Sci. **130**, L299 (1983).

[9]E. J. Van Loenen, J. E. Demuth, R. M. Tromp, and R. J. Hamers, Phys. Rev. Lett. **58**, 373 (1987).

[10]R. J. Wilson and S. Chiang, Phys. Rev. Lett. **58**, 369 (1987).

[11]M. Aono, Y. Hou, C. Oshima, and Y. Ishizawa, Phys. Rev. Lett. **49**, 567 (1982).

[12]M. Aono, Y. Hou, R. Souda, C. Oshima, S. Otavi, and Y. Ishizawa, Phys. Rev. Lett. **50**, 1293 (1983).

[13]T. L. Porter, C. S. Chang, U. Knipping, and I. S. T. Tsong, Phys. Rev. B **36**, 9150 (1987).

[14]C. S. Chang, U. Knipping, and I. S. T. Tsong, Nucl. Instrum. Methods Phys. Res., Sect. B **18**, 11 (1986).

[15]R. M. Tromp and J. F. Van der Veen, Surf. Sci. **133**, 159 (1983).

[16]M. Aono, R. Souda, C. Oshima, and Y. Ishizawa, Surf. Sci. **168**, 713 (1986).

[17]R. J. Wilson and S. Chiang, Phys. Rev. Lett. **59**, 2329 (1987).